

Fourier domain optical coherence tomography with ultralong depth range

Zhihua DING (✉), Yi SHEN, Wen BAO, Peng LI

State Key Lab of Modern Optical Instrumentation, Department of Optical Engineering, Zhejiang University, Hangzhou 310027, China

© Higher Education Press and Springer-Verlag Berlin Heidelberg 2015

Abstract The depth ranges of typical implementations of Fourier domain optical coherence tomography (FDOCT), including spectral domain OCT (SDOCT) and swept source OCT (SSOCT), are limited to several millimeters. To extend the depth range of current OCT systems, two novel systems with ultralong depth range were developed in this study. One is the orthogonal dispersive SDOCT (OD-SDOCT), and the other is the recirculated swept source (R-SS) interferometer/OCT. No compromise between depth range and depth resolution is required in both systems. The developed OD-SDOCT system realized the longest depth range (over 100 mm) ever achieved by SDOCT, which is ready to be modified for depth-encoded parallel imaging on multiple sites. The developed R-SS interferometer achieved submicron precision within a depth range of 30 mm, holding potential in real-time contact-free on-axis metrology of complex optical systems.

Keywords optical coherence tomography (OCT), virtually-imaged phased array (VIPA), orthogonal dispersion, swept source, light recirculation, parallel imaging, dimensional metrology

1 Introduction

Fourier domain optical coherence tomography (FDOCT) is an imaging modality that provides cross-sectional images of tissue/material microstructures by spectral analysis of the low-coherence interference fringe pattern. One typical implementation of the FDOCT is spectral domain OCT (SDOCT), where a grating is used as a dispersive component working together with one-dimensional (1-D) line-scan camera. Such a configuration of the SDOCT achieves moderate spectral resolution and sampling rate,

limiting the imaging range to several millimeters [1]. Another typical implementation of the FDOCT is swept source OCT (SSOCT), where the spectral resolution is mainly determined by the instantaneous bandwidth of the swept source. Most SSOCT systems adopt commercial available swept sources with moderate instantaneous line-width, and the depth ranges are also limited to several millimeters [2].

As Fourier-transform of real-valued spectral data introduces complex conjugate ambiguity in FDOCT, the measured sample generally has to be positioned at one side of the position of zero optical path difference (OPD) to avoid the overlapping of mirror images. Therefore, only one half of the depth range is available for FDOCT imaging. To restore the full depth range, many approaches have been proposed to remove the mirror image [3–5]. Techniques, such as interpixel shift to increase spectral sampling rate [1] and optical frequency comb to enhance spectral resolution [6], were proposed to increase the depth range but with moderate extension.

To substantially increase the depth range, an orthogonal dispersive OCT was first proposed by our group [7,8]. Alternatively, the method based on recirculating loops was also introduced by our group to extend the depth range well beyond the full-range limit [9]. In this paper, we introduced these two approaches proposed by our group for substantially extending the depth range of FDOCT systems. One is the orthogonal dispersive SDOCT (OD-SDOCT), and the other is the recirculated swept source (R-SS) interferometer/OCT. Tentative application in ultralong-range imaging and dimensional metrology were also presented.

2 System descriptions

2.1 OD-SDOCT

Conventional spectrometer in SDOCT uses grating as the

disperser in conjunction with 1-D charge coupled device (CCD). The spectral resolution is restricted by the spectrum range corresponding to one pixel size, and the spectral sampling rate is determined by the pixel number. The spectral sampling rate sets an upper limitation for the depth range according to the Nyquist theorem. To substantially increase the spectral resolution and sampling rate, the OD-SDOCT system based on orthogonal dispersion and two dimensional (2-D) CCD was proposed. The schematic diagram of the OD-SDOCT system is given in Fig. 1, where the conventional 1-D dispersive spectrometer in SDOCT is replaced by an orthogonal spectrometer. The orthogonal spectrometer based on combination of virtually-imaged phased array (VIPA) and grating was designed to disperse a broadband of 30 nm onto 2-D CCD with an ultrahigh spectral resolution of 2 pm. From the recorded 2-D orthogonal spectra, 1-D cascaded spectra were obtained and used for OCT image reconstruction.

In the OD-SDOCT system shown in Fig. 1, a super luminescent diode (SLD 371-HP, Superlum Diodes Ltd) with a full width at half maximum (FWHM) bandwidth of 45 nm centered at $\lambda_0 = 835$ nm is used as the low-coherence source. The emitted light from SLD is coupled into a fiber-based Michelson interferometer via a broadband optical circulator. A 90/10 fiber coupler is used as the

beam splitter. In the sample arm, the light is directed by a pair of X - Y galvanometer mirrors (6215H, Cambridge Technology) and then focused onto the sample by an objective lens with a focal length of 100 mm. The interference light returning from the reference arm and the sample arm is detected by the orthogonal spectrometer. In the orthogonal spectrometer, the interference light is first collimated by a collimator (beam-waist radius $W = 6.5 \mu\text{m}$) and focused into a line by a cylindrical lens (Thorlabs, LJ1653L1-B, $f_c = 200$ mm). The line-focused beam is incident onto the entrance window of a VIPA at an angle (θ_i) of 3° . The VIPA is a custom-built plane-parallel solid etalon, of which the back surface is coated with a partially reflective film ($r \approx 95\%$) and the front surface is coated with a reflective film ($R \approx 100\%$) except for an uncoated area used as the entrance window. The free spectrum range (FSR) of the VIPA is ~ 0.1 nm, mainly determined by its refractive index ($n = 1.50$) and geometrical thickness ($t = 2.40$ mm). The light after the VIPA is incident onto a grating (Wasatch Photonics, $d = 1/1200$ mm) with an angle (θ_g) of 30.1° . The orientation of the grating groove is normal to the focused line for orthogonal dispersion. The output spectra after the grating are focused by an imaging lens (Thorlabs, AC508-100-B, $f = 200$ mm) onto a 2-D CCD (UNIQU UP1830CL-12B, 1024×1024 pixels, pixel

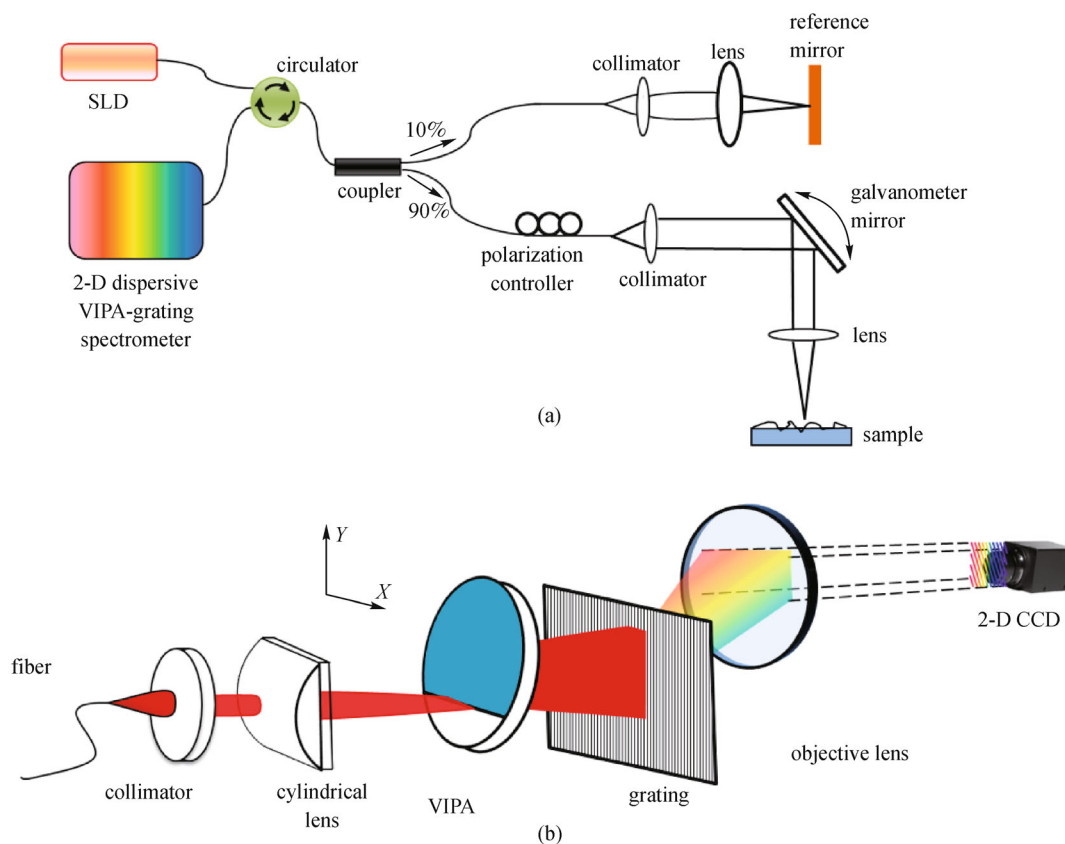


Fig. 1 (a) Schematic of OD-SDOCT system based on a virtually-imaged phased array (VIPA)-grating spectrometer; (b) detailed layout of the dispersive VIPA-grating spectrometer. SLD: super luminescent diode; CCD: charge coupled device

size of $6.45 \mu\text{m}$, frame rate of 30 Hz). The spectral data fetched by the CCD are transferred to a computer via a high-speed frame grabber board for data processing and image display.

2.2 R-SS interferometer/OCT

The spectral resolution in SSOCT is mainly determined by the instantaneous bandwidth of the swept source. For most commercial available swept sources, the depth ranges corresponding to their instantaneous line-widths is limited to several millimeters. To extend the depth range without increase of the coherence length of the swept source, we introduced the R-SS interferometer. The schematic of the R-SS interferometer is depicted in Fig. 2. With two recirculation loops implemented in two interfering arms with mismatched optical path lengths, the depth range can be cascaded by stepping the zero OPD points at light speed, a kind of similar to moving reference in time domain OCT. If lateral scanning is further performed, this R-SS interferometer is ready to be R-SSOCT.

The R-SS interferometer shown in Fig. 2 consists of a measurement interferometer and a reference interferometer sharing a common swept source. The reference interferometer is introduced to provide reference signals for all sweeps of the swept source. The commercial available swept source (HSL-2000, Santec Inc.) operating at a sweeping rate of 10 kHz is employed to provide a tuning range of 115 nm from 1267 to 1382 nm with instantaneous

coherence length around 12 mm. 90% of the output power from the swept source is sent into the measurement interferometer and directed into sample arm and reference arm through a 50/50 fiber coupler. Two recirculation loops are implemented in both sample arm and reference arm. The mismatched OPD between two recirculation loops is adjusted to be 16 mm through an optical delay line (OD). For every pass of the light through two recirculation loops, the zero OPD position of the measurement interferometer is shifted to the depth direction in the sample by half of the mismatched OPD, i.e., 8 mm. Interferences origin from different depth ranges of the sample are realized simultaneously without movement of reference mirror. To resolve these interference signals corresponding to different times of passage in two recirculation loops and thereafter encode them to depth information without ambiguity, two acousto-optic frequency shifters (AOFS1 and AOFS2, Brimrose Inc.) driven by voltage controlled oscillators under different frequencies (55 MHz for AOFS1, and 70 MHz for AOFS2) are used. To compensate for losses in two recirculation loops, two semiconductor optical amplifiers (SOA, Inphenix Inc.) are added. The interference signal from the measurement interferometer is detected by a balance detector (PDB450C, Thorlabs) with a bandwidth of ~ 150 MHz and sampled by one input channel of a 12-bit data acquisition (DAQ) card (PCI-5124, 200 Msample/s, National Instruments). 10% of the output power from the swept source is fed into the reference Mach-Zehnder interferometer (MZI). The OPD

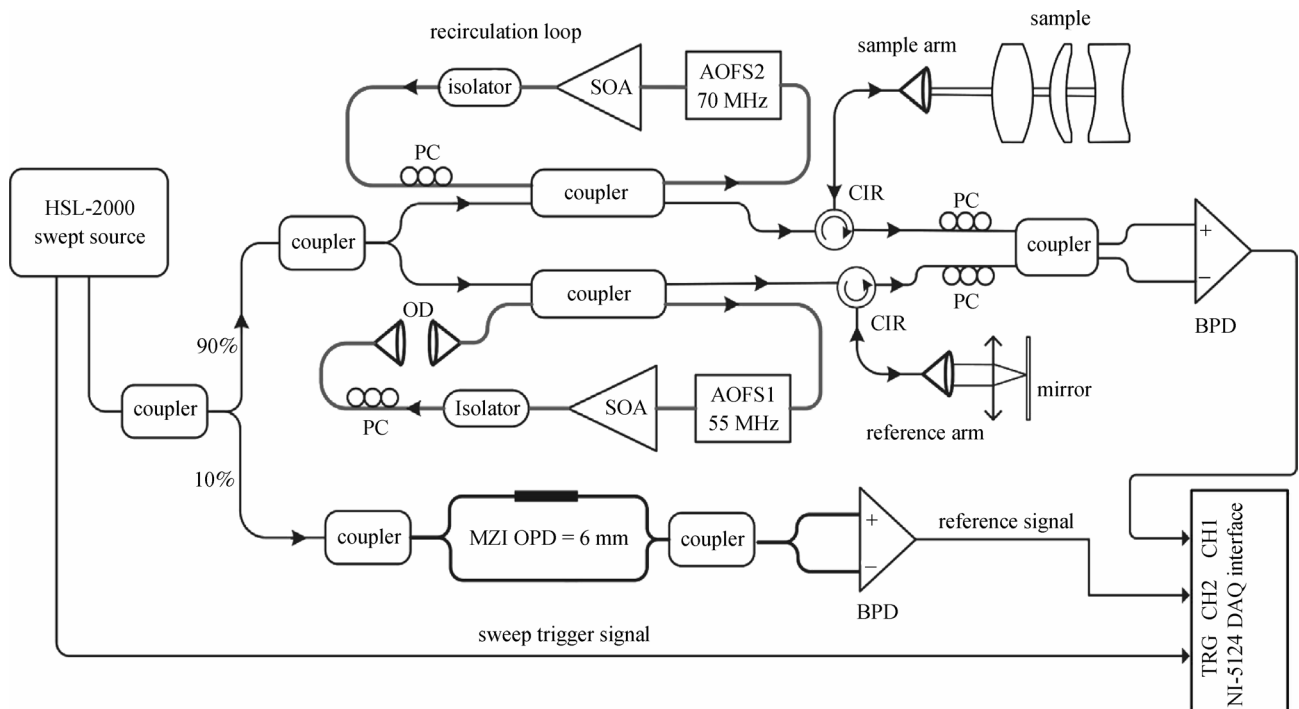


Fig. 2 Schematic of R-SS interferometer. Coupler: 50:50 fiber coupler; PC: polarization controllers; AOFS1, 2: acousto-optic frequency shifters; SOA: semiconductor optical amplifier; CIR: circulator; OD: optical delay line; MZI: Mach-Zehnder interferometer; BPD: balanced photodetector; CH1: channel 1; CH2: channel 2; TRG: trigger channel; DAQ: data acquisition

in the reference MZI is set to be 6 mm. Interference signal from the reference MZI is detected by another balance detector and sampled by another input channel of the DAQ card. The sweep trigger from the swept source is used as the trigger signal for the DAQ card.

3 Applications

3.1 OD-SDOCT

To validate the feasibility of the OD-SDOCT for high quality OCT imaging, a model eye (OEMI-7, Ocular Instruments, Inc., Bellevue, WA) with an overall length of 26 mm is first imaged by the OD-SDOCT system. The reconstructed OD-SDOCT image is shown in the left panel of Fig. 3, from which four zoomed views of the segmented ranges covering cornea, anterior lens, posterior lens, and retina are given in the middle of Fig. 3. For comparison, this model eye is also imaged sequentially at corresponding depth ranges by a conventional SDOCT system. As shown in the right panel of Fig. 3, these four images were obtained by stepping the reference mirror at four different positions. Because of its curved shapes and low reflectivities, the back scattered light intensity from the model eye is weak and hence low signal-to-noise ratio (SNR) in OD-SDOCT imaging, while it is comparable to conventional SDOCT imaging.

To demonstrate the OD-SDOCT system for ultralong-range imaging, a 102 mm long steel post connected to a post holder base is imaged and the reconstructed OCT image is shown in Fig. 4. An imaging range over 100 mm was realized, the longest depth range ever achieved by SDOCT. However, it should be emphasized that imaging range is different from imaging depth; the latter is usually restricted by scattering property of tissue to 1–3 mm. Therefore, such an ultralong-range OD-SDOCT system is directly useful in imaging of transparent medium or in profilometry.

To exploit the ultralong range for biomedical imaging, one candidate solution is depth-encoded parallel imaging as depicted schematically in Fig. 5. By depth multiplexing signals from multiple lateral locations into one ultralong-range A-scan, parallel measurements over a large field of view can be done simultaneously. As it inherits the merits of SDOCT in phase stability, the OD-SDOCT can be modified to perform multi-site phase measurements to obtain nanoscale displacement information from biologic samples, which could be very useful for monitoring fast cellular phenomena [10].

3.2 R-SS interferometer/OCT [9]

The measurement of center thicknesses and airgaps along its optical axis is crucial to a mounted optical system. The

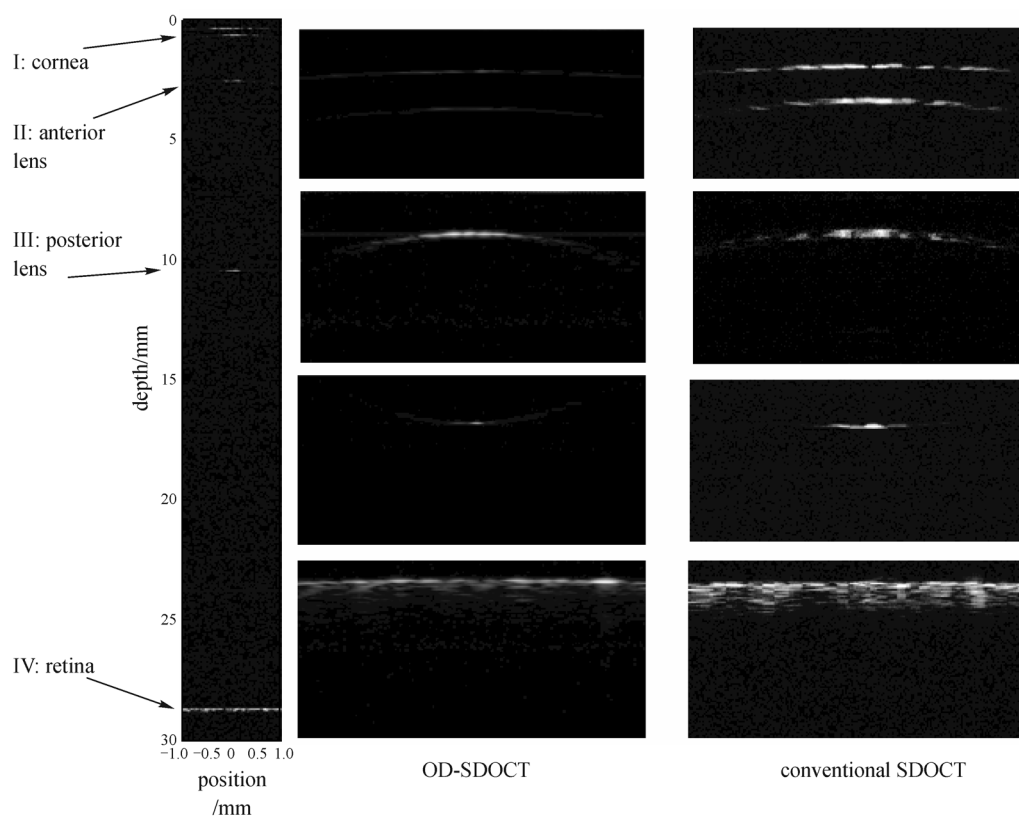


Fig. 3 Comparison imaging of a model eye by the OD-SDOCT system and conventional SDOCT system

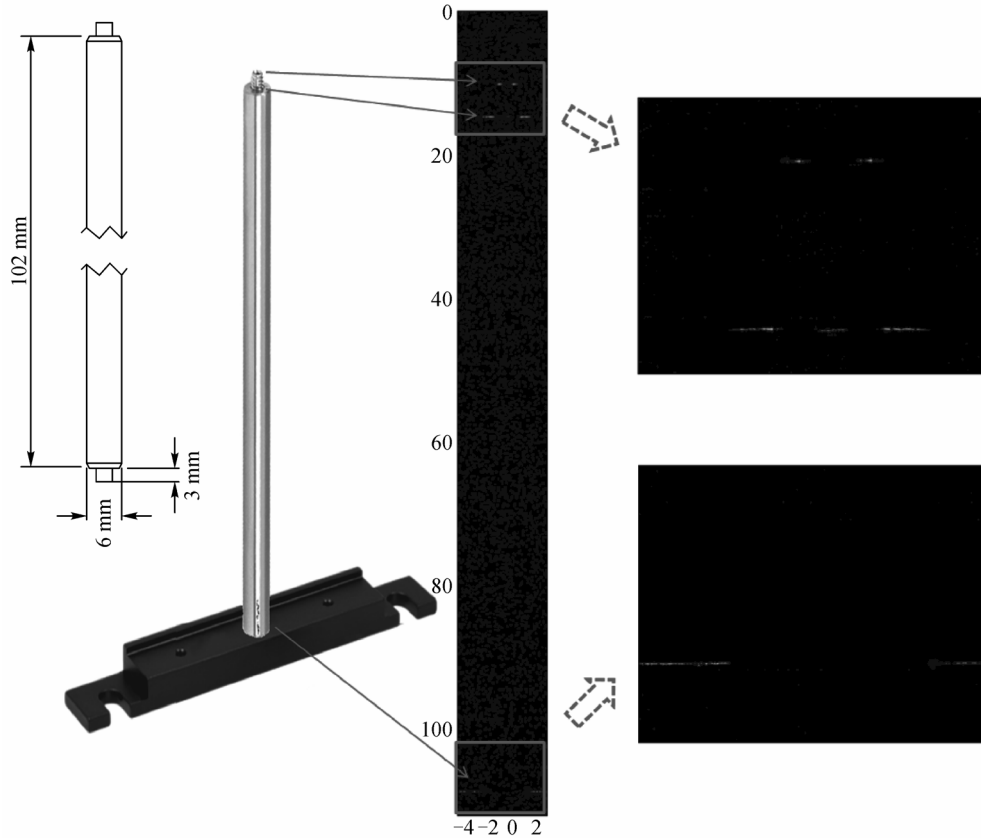


Fig. 4 Ultralong-range imaging of a steel post connected to a post holder base by the OD-SDOCT system

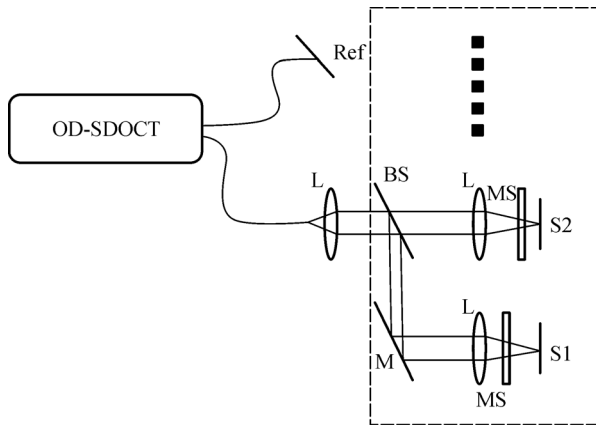


Fig. 5 Schematic of the depth-encoded OD-SDOCT for simultaneous multi-site imaging. Ref: reference arm; L: lens; BS: beam splitter; MS: multi-site; M: mirror; S1,2: sample lateral locations 1,2

developed R-SS interferometer is aimed to real-time dimensional metrology. To yield high precision of measurement, phase-sensitive approach based on phase-comparison between measurement signal and reference signal is adopted.

The feasibility of the R-SS interferometer for simulta-

neous measurement of multiple interfaces with extended range was confirmed by using a sample consisting of two glass plates with nominal optical thicknesses of 7.7 and 5.8 mm and separated from each other with a distance of 11.3 mm. As shown in the inset of the left panel of Fig. 6, the first surface of the glass plate is located at the position where noticeable visibility available in both circulations, while another three interfaces only has noticeable visibility within one circulation. Therefore, five profiles for the four interfaces are appeared in the frequency domain as demonstrated in the left panel of Fig. 6. After decoding from frequency domain to depth domain, this ambiguity in frequency domain can be removed. As shown in the right panel of Fig. 6, four profiles are reconstructed in depth domain corresponding to axial positions of 5.98, 13.66, 24.93 and 30.81 mm, respectively. From these axial positions, the optical thicknesses and the air gap distance of two plates were measured to be 7.68, 5.88 and 11.27 mm, in good agreement with the nominal values.

To evaluate the repeated precision along the extended depth range, measurements on optical thickness of a glass plate located at different positions along depth range were conducted. At each position, the measurements were repeated for 128 times. The nominal optical thickness of the glass plate was about 1.78 mm. The measured results are shown in Table 1. The standard deviation of the

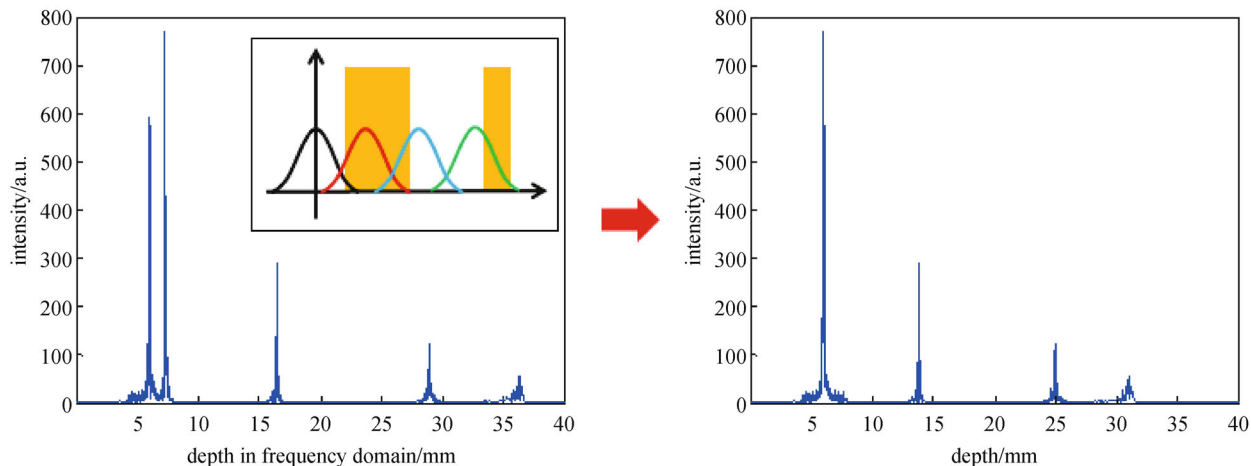


Fig. 6 Measured profiles for a sample consisting of four interfaces in frequency domain and depth domain

Table 1 Optical thickness measurements at different locations

location/mm	optical thickness/ μm	standard deviation/ μm
5	1779.5	0.02
10	1778.1	0.03
15	1779.3	0.14
20	1779.9	0.91
25	1779.5	0.36
30	1778.6	0.97

measured optical thickness for each position along the depth range from 5 to 30 mm was found to be within 1 μm .

4 Conclusions

Two novel systems with ultralong depth range were developed. The OD-SDOCT system realized an imaging depth over 100 mm, the longest depth range ever achieved by SDOCT. No compromise between depth range and depth resolution was required because of the tremendously increased spectral resolution and sampling of the orthogonal dispersive spectrometer. With faster frame rate of the 2-D detector, the OD-SDOCT with flexible parameter settings is a promising ultralong-range imaging modality. The R-SS interferometer achieved a cascaded depth range over 30 mm by virtual movement of zero OPD point at light speed through mismatched OPD between two circulation loops. Kind of similar to moving reference in time domain OCT, the R-SS interferometer makes no tradeoff between depth range and depth resolution. Submicron precision of distance measurement under unstable source with sweeping rate of 10 kHz was realized by phase comparison approach. The R-SS interferometer holds potential in real-time contact-free on-axis metrology of complex optical systems and is ready to be R-SSOCT for extended range imaging.

Acknowledgements We acknowledge financial supports from the National Natural Science Foundation of China (Grant Nos. 61275196, 61335003 and 61327007), Zhejiang Province Science and Technology Grant (No. 2012C33031), Zhejiang Provincial Natural Science Foundation of China (No. LY14F050007), and the Fundamental Research Funds for the Central Universities (No. 2014QNA5017).

References

1. Wang Z, Yuan Z, Wang H, Pan Y. Increasing the imaging depth of spectral-domain OCT by using interpixel shift technique. *Optics Express*, 2006, 14(16): 7014–7023
2. Huber R, Wojtkowski M, Taira K, Fujimoto J, Hsu K. Amplified, frequency swept lasers for frequency domain reflectometry and OCT imaging: design and scaling principles. *Optics Express*, 2005, 13(9): 3513–3528
3. Wojtkowski M, Kowalczyk A, Leitgeb R, Fercher A F. Full range complex spectral optical coherence tomography technique in eye imaging. *Optics Letters*, 2002, 27(16): 1415–1417
4. Wang K, Ding Z, Zeng Y, Meng J, Chen M. Sinusoidal B-M method based spectral domain optical coherence tomography for the elimination of complex-conjugate artifact. *Optics Express*, 2009, 17(19): 16820–16833
5. Davis A M, Choma M A, Izatt J A. Heterodyne swept-source optical coherence tomography for complete complex conjugate ambiguity removal. *Journal of Biomedical Optics*, 2005, 10(6): 064005
6. Bajraszewski T, Wojtkowski M, Szkulmowski M, Szkulmowska A, Huber R, Kowalczyk A. Improved spectral optical coherence tomography using optical frequency comb. *Optics Express*, 2008, 16(6): 4163–4176
7. Wang C, Ding Z, Mei S, Yu H, Hong W, Yan Y, Shen W. Ultralong-range phase imaging with orthogonal dispersive spectral-domain optical coherence tomography. *Optics Letters*, 2012, 37(21): 4555–4557
8. Bao W, Ding Z, Li P, Chen Z, Shen Y, Wang C. Orthogonal dispersive spectral-domain optical coherence tomography. *Optics Express*, 2014, 22(8): 10081–10090
9. Shen Y, Ding Z, Yan Y, Wang C, Yang Y, Zhang Y. Extended range

phase-sensitive swept source interferometer for real-time dimensional metrology. *Optics Communications*, 2014, 318: 88–94

10. Hendargo H C, Bower B A, Reinstein A S, Shepherd N, Tao Y K, Izatt J A. Depth-encoded spectral domain phase microscopy for simultaneous multi-site nanoscale optical measurements. *Optics Communications*, 2011, 284(19): 4847–4851



Dr. **Zhihua Ding** received his bachelor degree from Department of Optical Engineering at Zhejiang University (1989) and Ph.D. degree from Shanghai Institute of Optics and Fine Mechanics in China (1996). He was a Temporary Lecturer at Venture Business Laboratory of Shizuoka University in Japan (1998–2000) and a Senior Postdoctoral Fellow at Beckman Laser

Institute of University of California at Irvine (2000–2002). From 2002, he joined the Department of Optical Engineering at Zhejiang University. He was enrolled as a member of New Century Excellent Talents in University (2004). He is an editorial board member of “*Journal of Lasers, Optics & Photonics*”, “*Frontiers of Optoelectronics*”, “*Journal of Innovative Optical Health Sciences*”, an associated editor of “*Acta Laser Biology Sinica*”, and an executive member of the editorial board for “*Chinese Journal of Lasers*”. His research aims to investigate light/tissue (cell) interactions at micro to nano scale for high resolution and novel contrast, develop optical instruments for biomedical applications and fundamental researches. His current research foci are *in vivo* optical imaging and other *in vitro* optical method, especially in optical coherence tomography.



Yi Shen is currently working toward the Ph.D. degree in optical engineering under Prof. Zhihua Ding. He received his bachelor degree in optical information science and technology and master degree in optical engineering from Fujian Normal University in 2007 and 2011, respectively. His current research focuses on the development of non-invasive, high-resolution, high-speed

optical imaging technology, including extra-long imaging range swept source optical coherence tomography (SS-OCT), phase sensitive SS-OCT, and endoscopic SS-OCT.



Wen Bao received his bachelor degree from Department of Optical Engineering at Zhejiang University (2013), where he is currently working toward the Ph.D. degree in optical engineering under Prof. Zhihua Ding. His current research focuses on optical coherence tomography (OCT) and optical measurement, especially orthogonal dispersive spectral-domain optical coherence tomography (OD-SDOCT).



Dr. **Peng Li** is currently an Associate Professor of Optical Engineering at the Zhejiang University. Dr. Li received his B.E. degree in optoelectronic information engineering and Ph.D. degree in optical engineering from Nanjing University of Science and Technology in 2005 and 2010, respectively. After three years’ post-doctoral research training at the University of Washington, Seattle, USA, he joined Zhejiang University in 2013. His current research interests include the development of non-invasive, high-resolution, high-speed optical biomedical imaging technology: optical coherence tomography (OCT), OCT-based angiography, OCT-based elastography, laser speckle, photoacoustic imaging, and their applications in neurology, ophthalmology, dermatology and tumor. He has published more than 15 peer-reviewed SCI journal articles and more than 10 international conference papers. The significance of his work is further emphasized by peer selection of his article for a special SPIE recommendation (SPIE R&D Highlights by Lihong Wang in SPIE Professional April 2013, <http://spie.org/x93157.xml>).